

# Inhibition mechanism and corrosion protection of mild steel in hydrochloric acid using 2-hydroxynaphthaldehyde thiosemicarbazone (2HNT): Experimental and theoretical analysis

A.A. Zainulabdeen,<sup>1</sup> Z.A. Betti,<sup>2</sup> D.M. Jamil,<sup>3</sup> A.M. Mustafa,<sup>1</sup> F.F. Sayyid,<sup>1</sup> M.M. Hanoon,<sup>1</sup> T.S. Gaaz<sup>4</sup>  and A. Alamiery<sup>5,6</sup> \*

<sup>1</sup>Department of Materials Engineering, University of Technology, Iraq, P.O. Box: 10001, Baghdad, Iraq

<sup>2</sup>Technical Engineering College, Middle Technical University, P.O. Box: 10001, Baghdad, Iraq

<sup>3</sup>Department of Chemistry, College of Science, Al-Nahrain University, Baghdad, Iraq

<sup>4</sup>Air Conditioning and Refrigeration Techniques Engineering Department, College of Engineering and Technologies, Al-Mustaqbal University, 51015, Babylon, Iraq

<sup>5</sup>Energy and Renewable Energies Technology Center, University of Technology, Iraq, P.O. Box: 10001, Baghdad, Iraq

<sup>6</sup>Department of Chemical and Process Engineering, Faculty of Engineering and Build Environment, Universiti Kebangsaan Malaysia, P.O. Box: 43600, Bangi, Selangor, Malaysia

\*E-mail: [dr.ahmed1975@gmail.com](mailto:dr.ahmed1975@gmail.com)

## Abstract

This study explores the inhibitory properties of 2-hydroxynaphthaldehyde thiosemicarbazone (2HNT) on mild steel corrosion in 1 M hydrochloric acid. The investigation of adsorption and inhibition mechanisms employed weight loss analysis, scanning electron microscopy (SEM), and density functional theory (DFT) techniques. Adsorption parameters were derived using various theoretical approaches. Optimal inhibitive efficacy, reaching 93.88%, was observed at a concentration of 500.0 ppm for the inhibitor during a 10-hour immersion period at 303 K. The study further examined the impact of immersion durations (5, 10, 24, and 48 hours) and inhibitor concentrations (100–1000 ppm) at 303 K, revealing 10 hours as the optimum immersion time. Inhibition efficiency increased with rising inhibitor concentration and remained steady beyond 10 hours up to 48 hours. Temperature effects were explored for different inhibitor concentrations, with 10 hours identified as the optimal immersion time. The Langmuir adsorption isotherm model was employed to elucidate the adsorption inhibition mechanism. Changes in activation energy values indicated distinct interactions between inhibitor molecules and the mild steel surface. Scanning electron microscopy analyses confirmed inhibitor molecule adsorption and the formation of a protective film on the mild steel surface. The mild steel-inhibitor interaction was scrutinized through DFT, revealing a minimal energy gap between the highest occupied molecular orbital (HOMO) and the lowest unoccupied molecular orbital (LUMO). The experimental and theoretical findings demonstrated congruence, affirming

the efficacy of 2-hydroxynaphthaldehyde thiosemicarbazone as a corrosion inhibitor for mild steel in hydrochloric acid.

Received: January 6, 2024. Published: May 22, 2024

doi: [10.17675/2305-6894-2024-13-2-16](https://doi.org/10.17675/2305-6894-2024-13-2-16)

**Keywords:** *thiosemicarbazone, hydroxynaphthaldehyde, inhibition efficiency, corrosion mechanisms.*

## 1. Introduction

Mild steel, owing to its advantageous mechanical properties and affordability, holds a prominent position as a widely used material across various industrial sectors [1–3]. However, its susceptibility to corrosion in aggressive environments, particularly hydrochloric acid (HCl) solutions, presents a significant challenge to its longevity and structural integrity. HCl finds extensive application in processes like acid pickling and descaling, which contribute significantly to the accelerated corrosion of mild steel surfaces [4–8]. To mitigate corrosion-induced degradation, researchers have actively explored various strategies, with a particular focus on corrosion inhibitors. These inhibitors can be broadly classified into inorganic and organic categories [4–6]. Organic inhibitors, owing to their versatility and ability to form protective layers on metal surfaces, have garnered significant attention in recent years [9–17]. Organic compounds containing heteroatoms like N, S, P, X (halogen), and O have been recognized for their potential as effective corrosion inhibitors. Among these organic compounds, Schiff bases, characterized by the general formula  $R-C=N-R'$  (where R and R' represent aryl, alkyl, cycloalkyl, or heterocyclic groups), have emerged as promising candidates for corrosion protection [18–20]. One specific type of Schiff base, thiosemicarbazone derivatives, possesses unique structural features with amine and thion groups containing N and S heteroatoms, providing ideal sites for chemisorption on metal surfaces. These features contribute to their effectiveness as corrosion inhibitors [21–23]. While existing research demonstrates the potential of Schiff bases as corrosion inhibitors, there are limitations that necessitate further exploration. For instance, the Schiff base 2-(2-oxoindolin-3-ylidene) hydrazinecarbothioamide (OHB) exhibits a significant corrosion inhibition efficiency reaching 96.7% at a concentration of 0.5 mM and 303 K. However, its performance suffers with extended immersion times and increasing temperatures, hindering its broader applicability [24]. Similarly, promising alternatives like 2,2'-(1,4-phenylenebis(methanylylidene)) bis(*N*-(3-methoxyphenyl) hydrazinecarbothioamide) (PMBMH) face limitations in terms of maintaining efficiency over longer durations and under elevated temperatures [25].

The realm of Schiff bases and their application as corrosion inhibitors for mild steel in acidic environments has witnessed significant advancements in recent years. Researchers have continuously explored novel Schiff base derivatives with diverse structural features, aiming to enhance their corrosion inhibition efficiency and overcome limitations associated

with existing compounds. Here, we highlight some noteworthy recent findings and identify lingering gaps in this domain:

- *Enhancing efficacy through structural modifications:* Studies have demonstrated how strategic modifications in the structure of Schiff bases can significantly impact their performance. The incorporation of electron-donating groups (EDGs) onto the Schiff base backbone has been shown to enhance adsorption onto the metal surface, thereby improving inhibition efficiency. For instance, a recent study by [51] reported the development of Schiff bases derived from cinnamaldehyde and various aromatic amines. These inhibitors exhibited superior performance compared to their unsubstituted counterparts, attributing this improvement to the presence of EDGs on the aromatic rings.
- *Exploring synergistic effects and green alternatives:* The investigation of synergistic effects between Schiff bases and other corrosion inhibitors has emerged as a promising approach. Combining Schiff bases with inorganic or other organic inhibitors can lead to a more robust protective layer, potentially surpassing the individual efficacy of each component. For example, a study by [52] demonstrated that the combination of a Schiff base derived from 2-aminothiazole and potassium iodide exhibited superior corrosion inhibition compared to either compound alone. Additionally, the growing emphasis on sustainable practices has led to the exploration of eco-friendly Schiff bases derived from natural sources. Research by [53] reported the development of Schiff bases synthesized from plant extracts, demonstrating their potential as effective and environmentally benign corrosion inhibitors for mild steel.

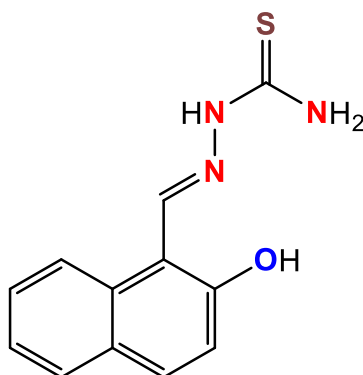


**Figure 1.** The chemical structure of 2HNT.

Despite the significant progress, certain knowledge gaps persist in the field of Schiff base corrosion inhibitors. A deeper understanding of the structure-property relationship, particularly the correlation between specific functional groups and their influence on inhibition behavior, remains crucial. Additionally, a more comprehensive assessment of the long-term stability and environmental impact of these inhibitors is necessary for their wider acceptance. By investigating the corrosion inhibition potential of 2HNT (Figure 1) and employing a combination of experimental and theoretical techniques, our study aims to contribute to closing these knowledge gaps. We anticipate that our findings will shed light

on the adsorption and inhibition mechanisms of 2HNT, paving the way for the development of more effective and sustainable corrosion protection strategies for mild steel in acidic environments. This study aligns with the ongoing efforts to explore novel and efficient Schiff bases, potentially surpassing the limitations of existing inhibitors and addressing the evolving needs of the field.

## 2. Experimental

### 2.1. Mild steel sampling

Mild steel coupons with a composition of 0.21% Carbon, 0.09% Phosphorus, 0.05% Manganese, 0.038% Silicon, 0.01% Aluminum, 0.05% Sulfur, and the remainder Iron were employed in the study. Prior to each experimental run, the coupons underwent meticulous preparation, involving division into distinct sections, abrasion with sandpaper, degreasing with acetone, and oven drying to shield them from ambient humidity [51, 52]. Subsequently, the prepared coupons were suspended using wire in a beaker containing 250 mL of 1 mol·L<sup>-1</sup> HCl (37%), both in the presence and absence of 2HNT as a tested inhibitor. After corrosion exposure, each sample underwent a thorough cleansing process involving double-distilled water, methyl alcohol immersion to eliminate 2HNT particles and chlorine residuals, acetone immersion, and final drying in an oven, followed by weight measurements.

### 2.2. Weight loss analyses

Weight loss analysis was conducted on mild steel coupons in a 1 mol·L<sup>-1</sup> HCl medium, with and without the presence of 2HNT. Initial measurements of the polished coupons were recorded, and the coupons were immersed in the analysis liquid using a glass clamp in triplicate, under varying concentrations of 2HNT (100, 200, 300, 400, 500, and 1000 ppm). Post-immersion, the coupons were reweighed, rinsed, and dried. The impact of time on inhibition efficiency at different inhibitor concentrations was investigated over periods of 1, 5, 10, 24, and 48 hours. Additionally, the temperature effect on inhibition efficacy at various concentrations was studied within the range of 303–333 K. The corrosion rate ( $C_R$ ; mm·y<sup>-1</sup>) and inhibition efficiency ( $IE\%$ ) were determined using Equations 1 and 2, respectively [51–54].

$$C_R = \frac{87.6W}{adt} \quad (1)$$

$$IE\% = \frac{C_R^0 - C_R}{C_R^0} \cdot 100 \quad (2)$$

where  $W$  is the loss in coupon weight (mg/cm<sup>2</sup>),  $a$  represents the immersion area,  $d$  refers to the coupon density,  $t$  is the immersion period, and  $C_R^0$  and  $C_R$  represent the rates of corrosion

without and with the corrosion inhibitor, respectively. To ensure the accuracy of the weight loss results, mild steel samples were weighed three times.

### 2.3. Surface morphology investigation

Surface morphology of the coupons exposed to 1 mol·L<sup>-1</sup> HCl, both in the presence and absence of 2HNT, was examined at room temperature using a scanning electron microscope (SEM). This analysis aimed to scrutinize the changes in mild steel surface characteristics before and after weight loss measurements. The SEM used for this purpose was the Scanning Electron Microscope (TM1000 Hitachi Tabletop Microscope SEM). Coupons were subjected to a 5-hour exposure to 1 mol·L<sup>-1</sup> HCl solution with and without the optimum inhibitor concentration. Subsequently, the coupons were removed, washed with deionized water, dried, and scrutinized using SEM.

### 2.4. Theoretical investigations

To gain insights into the inhibitor's performance and identify critical factors influencing inhibitive efficacy, quantum chemical computations were performed using Density Functional Theory (DFT). Becke's three-parameter hybrid functional with the LYP correlation functional (B3LYP) was employed to study the electronic characteristics of the inhibitor molecules [55, 56]. Ionization energy ( $I$ ), electronic affinity ( $A$ ), electronegativity ( $\chi$ ), hardness ( $\eta$ ), and number of electrons transferred ( $\Delta N$ ) were determined using the highest energy MO (HOMO) and lowest energy MO (LUMO). The iron work function ( $\phi$ ) was considered as 4.82 eV, and the iron hardness was evaluated at 0 as  $I=A$  [55–58]. The quantum parameters were computed based on Equations 3–7.

$$I = -E_{\text{HOMO}} \quad (3)$$

$$A = -E_{\text{LUMO}} \quad (4)$$

$$\chi = 0.5(I + A) \quad (5)$$

$$\eta = 0.5(I - A) \quad (6)$$

$$\Delta N = \frac{\phi - \chi_{\text{inh}}}{2(\eta_{\text{Fe}} + \eta_{\text{inh}})} \quad (7)$$

where:

- $I$  is the ionization energy.
- $E_{\text{HOMO}}$  is the energy of the highest occupied molecular orbital.
- $A$  is the electronic affinity.
- $E_{\text{LUMO}}$  is the energy of the lowest unoccupied molecular orbital.
- $\chi$  is the electronegativity.
- $\eta$  is the hardness.
- $\Delta N$  is the transferred electrons fraction.

### 3. Result and Discussion

#### 3.1. Effect of inhibitor concentration

The investigation into the effect of inhibitor concentration on the corrosion rate of mild steel in a hydrochloric acid solution revealed compelling insights, particularly at a 10-hour immersion time. In the absence of the studied inhibitor, the corrosion rate exhibited a notably high value, indicative of the aggressive nature of the corrosive environment. However, with the introduction of the inhibitor, a marked reduction in the corrosion rate was observed, indicating the inhibitive effectiveness of the studied compound. Figure 2 illustrates the impact of different concentrations of 2HNT on the weight loss of mild steel after 10 hours of immersion in a  $1.0 \text{ mol}\cdot\text{L}^{-1}$  HCl solution at a temperature of 303 K. The data highlights the corrosion inhibitory effects of 2HNT on mild steel under these specific conditions [59, 60]. The data presented in the Figure 2 unequivocally illustrates the inverse relationship between inhibitor concentration and the corrosion rate of mild steel. At lower concentrations (0–200 ppm), a gradual reduction in the corrosion rate is evident, reflecting the increasing effectiveness of the inhibitor in mitigating corrosion. This reduction can be attributed to enhanced adsorption of inhibitor molecules on the mild steel surface, leading to improved surface coverage [61, 62]. As the inhibitor concentration continues to rise beyond 200 ppm, a more pronounced decline in the corrosion rate is observed. The inhibitive efficiency, represented as the percentage reduction in the corrosion rate, shows a remarkable ascent. Notably, at 500 ppm and 1000 ppm, the corrosion rate is significantly suppressed, reaching values of 3.8 mm/y and 2.7 mm/y, respectively.

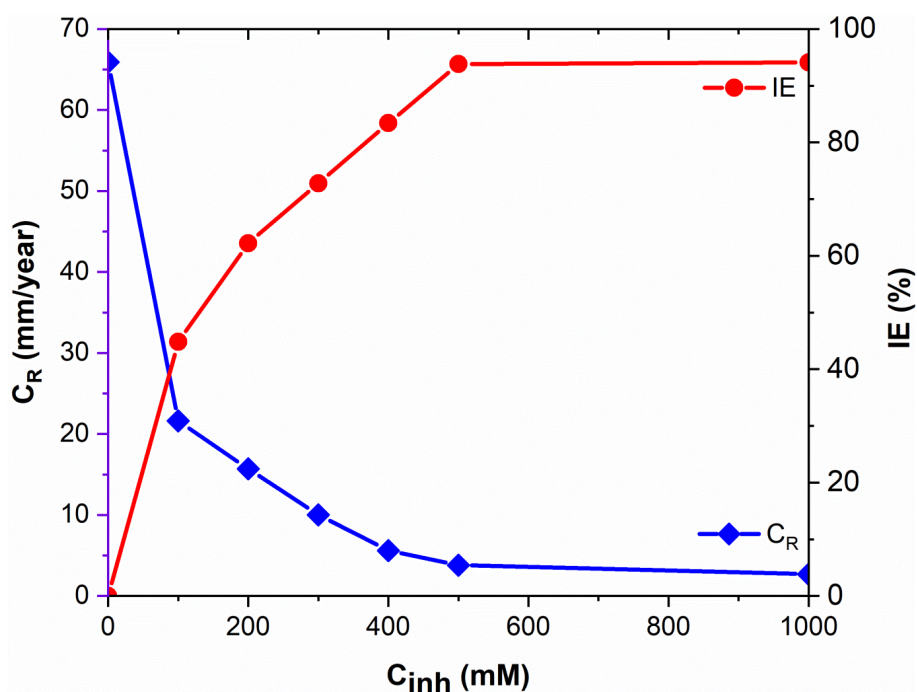


**Figure 2.** Effects of 2HNT concentrations on corrosion rate and inhibition efficiency of mild steel in  $1.0 \text{ mol}\cdot\text{L}^{-1}$  HCl at 10 hours immersion time and 303 K.

The observed trend aligns with the anticipated behavior of corrosion inhibitors, where a higher concentration fosters greater adsorption, creating a protective layer on the metal surface. The substantial increase in inhibition efficiency, reaching 93.8% and 94.1% at 500 ppm and 1000 ppm, respectively, underscores the remarkable effectiveness of the studied inhibitor in curbing mild steel corrosion in hydrochloric acid.

### 3.2. Effect of immersion time

The experimental investigation delving into the effect of immersion time on the corrosion behavior of mild steel in a  $1.0 \text{ mol}\cdot\text{L}^{-1}$  HCl solution has unearthed critical insights into weight loss, inhibitive efficacy, and surface coverage. Figure 3 outlines the variations in weight loss over different exposure periods, shedding light on the dynamic nature of the corrosion process [63, 64].

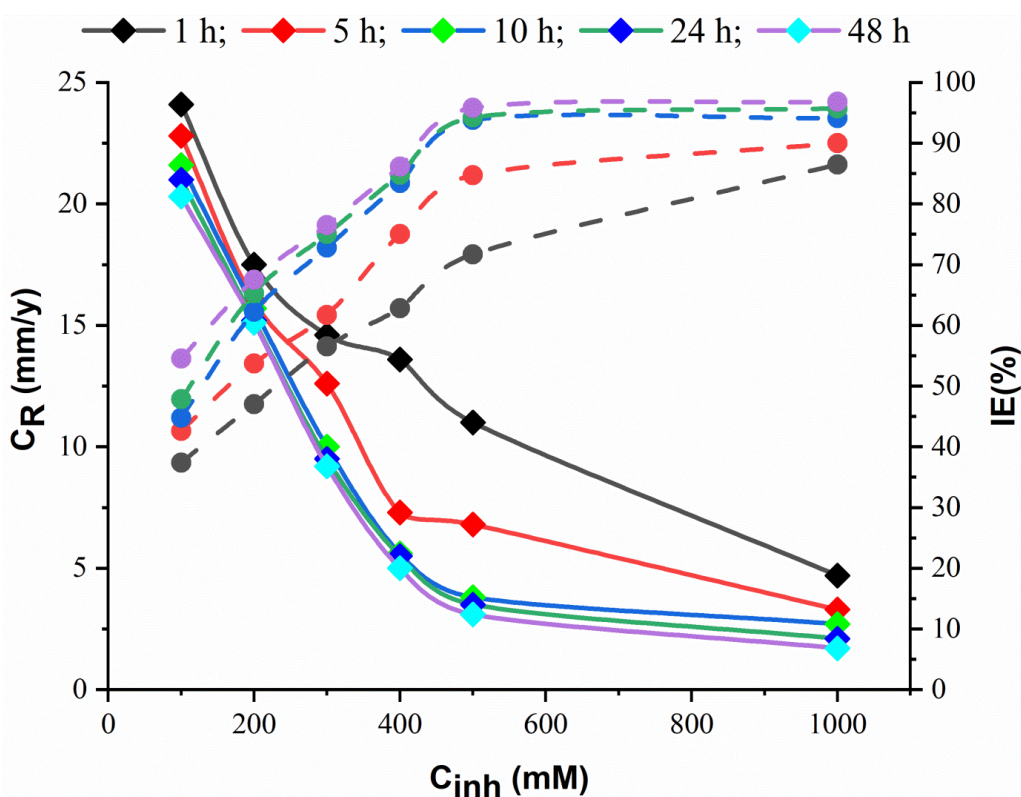


**Figure 3.** Impact of 2HNT concentrations on corrosion rate and inhibition efficiency of mild steel in  $1.0 \text{ mol}\cdot\text{L}^{-1}$  HCl at different immersion times and 303 K.

The examination of different immersion times (1, 5, 10, 24, and 48 hours) provides a comprehensive understanding of the temporal evolution of corrosion processes on mild steel in the presence of the inhibitor 2HNT [65]. The weight loss results, as presented in Figure 3, indicate a gradual decrease in the corrosion rate with increasing exposure time for the tested coupons. This decline is indicative of the inhibitor's persistent influence on reducing the metal's susceptibility to corrosion over extended periods [66]. The inhibited specimens

exhibit lower weight loss values compared to their uninhibited counterparts, illustrating the protective effect of 2HNT [67]. The inhibitive efficacy, represented as the percentage reduction in corrosion rate, displays a nuanced relationship with immersion time. Notably, the inhibitive efficacy increases slightly with prolonged exposure time for all concentrations of the tested inhibitor. This behavior suggests that the inhibitor molecules (2HNT) continue to interact with environmental species, leading to sustained inhibition. However, it's crucial to acknowledge that prolonged exposure may also result in the gradual depletion or desorption of inhibitor molecules due to complex interactions with the mild steel surface [68, 69].

At the optimum inhibitor concentration of 500 ppm, the inhibition efficiency reaches 93.8% after 10 hours of immersion. Interestingly, the highest inhibition activity of 96.8% is achieved after 48 hours of immersion, with a concentration of 1000 ppm of 2HNT. It's worth noting that concentrations exceeding 1000 ppm show no significant difference in inhibition activity within the examined range, indicating a potential saturation effect [70]. This observed trend may be attributed to intricate interactions between the inhibitor molecules and the mild steel surface, leading to the formation of a protective film. The results suggest that 2HNT demonstrates remarkable and sustained inhibitive performance over an extended exposure period, offering promising prospects for its application as an effective corrosion inhibitor for mild steel in aggressive acidic environments [71]. In summary, the results affirm that the studied inhibitor concentration plays a pivotal role in determining its inhibitive efficacy, showcasing a promising potential for the compound as an efficient corrosion inhibitor for mild steel in aggressive acidic environments.

### 3.3. Effect of temperature

The investigation into the influence of temperature on the corrosion rate and inhibition efficiency provides valuable insights into the dynamic behavior of mild steel in a  $1.0 \text{ mol}\cdot\text{L}^{-1}$  HCl solution. The obtained outcomes, detailed in Figure 4, reveal notable trends in the corrosion process under varying temperature conditions [72]. The examination of temperature's impact on corrosion behavior reveals a noteworthy inverse relationship between temperature and the corrosion rate. Generally, the corrosion rate decreases with an increase in temperature, as illustrated in Figure 4. This phenomenon can be attributed to enhanced chemical interactions and the improved solubility of oxygen at elevated temperatures, leading to more favorable corrosion reactions [73, 74]. However, the temperature effect also manifests in the inhibitive efficacy, showcasing a negative correlation. As temperature rises, there is an increase in dynamic energy for the tested inhibitor molecules. This elevated energy state, in turn, impacts the protective layer formed on the mild steel surface, potentially leading to a reduction in inhibition efficiency. This observation is consistent with the dynamic nature of inhibitor-metallurgic interactions, where temperature plays a crucial role in altering the energy landscape of the system [75, 76]. Despite the negative impact on inhibition efficacy, an interesting trend emerges with the increase in temperature, particularly at 10 hours of immersion time and an inhibitor

concentration of 1000 ppm. In this scenario, the inhibition efficiency rises from 94.1% at 303 K to 97.1% at 333 K, suggesting a complex interplay of temperature, inhibitor concentration, and exposure time [77–81].

In conclusion, the temperature effect on the corrosion behavior of mild steel in hydrochloric acid solution is intricate, involving both the reduction in corrosion rate due to enhanced chemical interactions and the simultaneous negative impact on inhibition efficiency. The results emphasize the importance of carefully considering temperature conditions when assessing the performance of corrosion inhibitors, as they play a dual role in influencing the corrosion process.

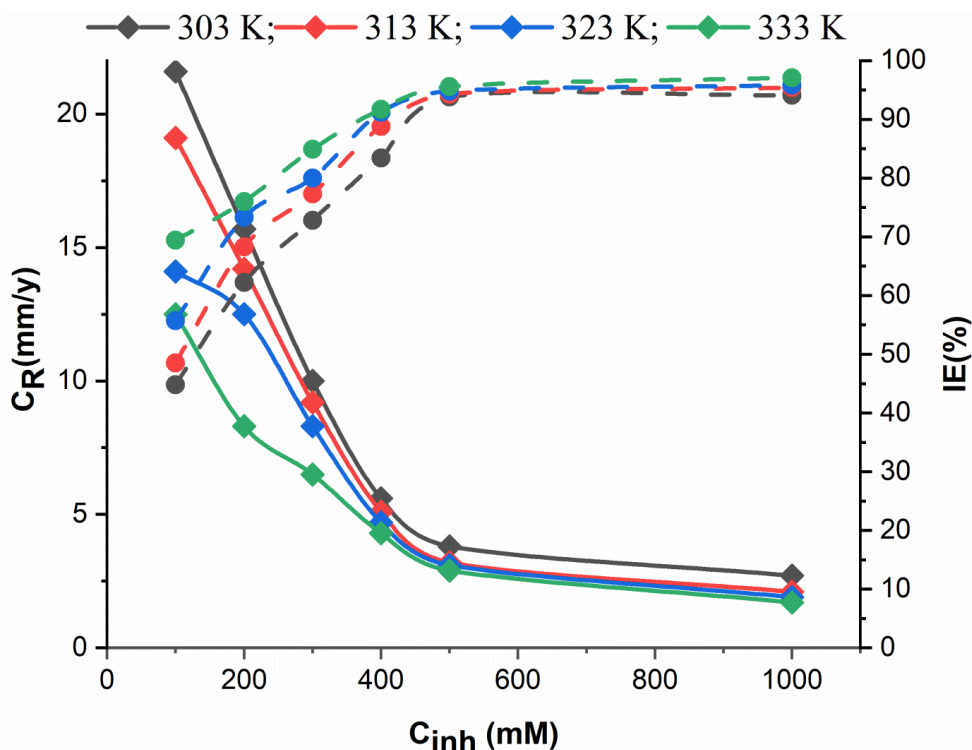


**Figure 4.** Impact of 2HNT concentrations on corrosion rate and inhibition efficiency of mild steel in  $1.0 \text{ mol}\cdot\text{L}^{-1}$  HCl at different temperature and 10 hours immersion time.

### 3.4. Adsorption isotherm studies

Adsorption isotherms play a crucial role in elucidating the performance of organic adsorbent-type inhibitors, providing insights into the mechanisms of organic electrochemical reactions. In this study, Langmuir, Temkin, and Frumkin isotherms were assessed to understand the relationship between surface coverage ( $\theta$ ) and bulk concentration, with Langmuir emerging as the most descriptive model [82–85]. The Langmuir isotherm, frequently employed to characterize adsorption behavior, demonstrated an excellent fit for the investigated 2HNT. The straight-line plot obtained by plotting  $\log C/\theta$  against  $\log$  inhibitor concentration ( $C$ ) at 303 K (as depicted in Figure 5) supports Langmuir's suitability in describing the adsorption behavior.

Langmuir isotherm is mathematically represented by the equation 8:

$$\frac{C_{\text{inh}}}{\theta} = C_{\text{inh}} + K_{\text{ads}}^{-1} \quad (8)$$

Here,  $C_{\text{inh}}$  represents the inhibitor concentration, and  $\theta$  is the surface coverage, defined as the fraction of the surface treated by inhibitor molecules.

The surface coverage ( $\theta$ ) can be calculated using the inhibition efficiency ( $IE$ ) values obtained from weight loss measurements, based on Equation 9:

$$IE\% = \frac{C_{\text{R}}^0 - C_{\text{R}}}{C_{\text{R}}^0} \quad (9)$$

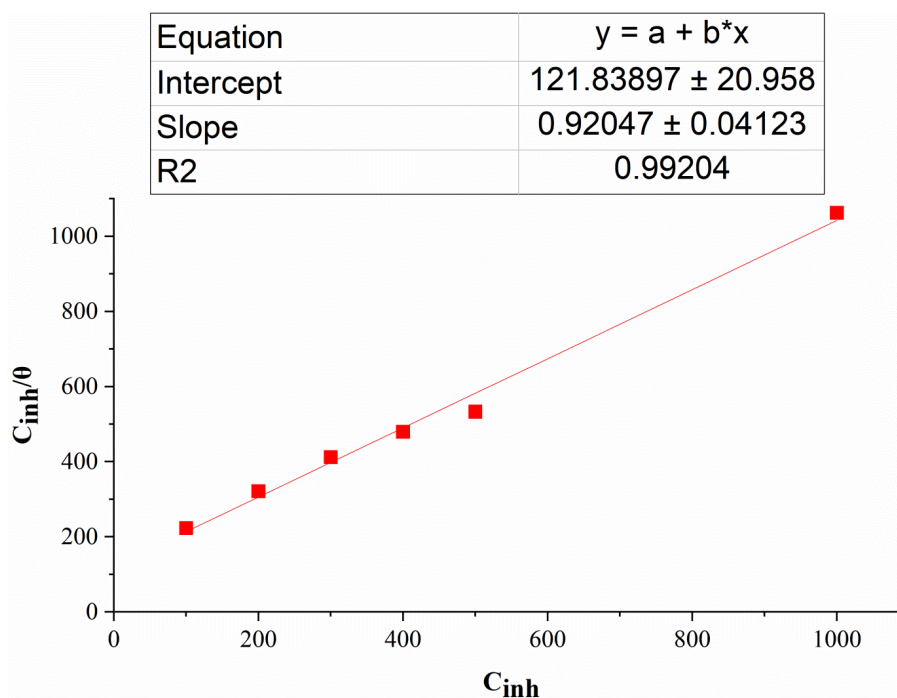


**Figure 5.** Langmuir adsorption isotherm for 2HNT on mild steel surface in  $1.0 \text{ mol} \cdot \text{L}^{-1}$  HCl at 303 K.

The straight-line plot of  $C_{\text{inh}}/\theta$  against  $C_{\text{inh}}$  achieved at 303 K validates Langmuir's adherence to the adsorption process. The linear regression coefficient close to unity reinforces the model's appropriateness compared to other isotherm models. The adsorption equilibrium constant ( $K_{\text{ads}}$ ), determined from the intercept of the straight line (Figure 5), signifies the affinity between the adsorbate and adsorbent. A higher  $K_{\text{ads}}$  value indicates superior adsorption, correlating with more reliable inhibition efficiency [86–90]. The relationship between adsorption free energy ( $\Delta G_{\text{ads}}^0$ ) and the adsorption equilibrium constant is given by the equation 10 [86]:

$$\Delta G_{\text{ads}}^0 = -RT \ln(55.5 K_{\text{ads}}) \quad (10)$$

In this equation,  $R$  is the universal gas constant,  $T$  is the absolute temperature, and  $K_{\text{ads}}$  is the adsorption equilibrium constant. The negative value of  $\Delta G_{\text{ads}}^0$  indicates spontaneity in the adsorption process, signifying efficient adsorption of inhibitor molecules on the surface of mild steel [87]. It is evident that the adsorption free energy ( $\Delta G_{\text{ads}}^0$ ) serves as a key indicator in delineating the nature of adsorption interactions. A  $\Delta G_{\text{ads}}^0$  with a value less than or equal to  $-20$  kJ/mol suggests physisorption, signifying a relatively weaker interaction where inhibitor molecules adhere to the surface through physical forces. On the other hand, an adsorption free energy with an extremely negative value exceeding  $-40$  kJ/mol implies chemisorption. This is indicative of a more profound interaction mechanism, involving the formation of coordination bonds between the unoccupied d-orbitals of iron atoms on the coupon surface and the unshared pairs of electrons present in the tested inhibitor molecules [88]. The range between  $-20$  kJ/mol and  $-40$  kJ/mol represents a transitional region where a mixed interaction type, encompassing both physisorption and chemisorption, is likely to occur. This nuanced understanding of adsorption energetics provides valuable insights into the diverse modes of interaction between the inhibitor and the metal surface, contributing to a comprehensive comprehension of the inhibition mechanism.

The calculated value of  $\Delta G_{\text{ads}}^0$  as  $-34.3$  kJ/mol suggests a mixed interaction type involving both chemisorption and physisorption. The negative value aligns with the spontaneity of the adsorption process, while the magnitude implies a combination of coordination bonds between unoccupied d-orbitals of iron atoms on the coupon surface and unshared pairs of electrons of the tested inhibitor molecules. In conclusion, the adsorption isotherm studies highlight the effectiveness of Langmuir isotherm in characterizing the adsorption behavior of 2HNT on mild steel in hydrochloric acid [89]. The mixed interaction type, incorporating chemisorption and physisorption, adds depth to the understanding of the inhibition mechanism, emphasizing the potential of 2HNT as a corrosion inhibitor with diverse interaction modes.

### 3.5. Surface analysis

Surface analysis provides a visual insight into the protective capabilities of the 2HNT inhibitor on mild steel exposed to a  $1.0 \text{ mol}\cdot\text{L}^{-1}$  HCl solution. Figures 6a and 6b depict the observable differences in the tested coupon surface without and with the presence of 2HNT after a 5-hour exposure period.

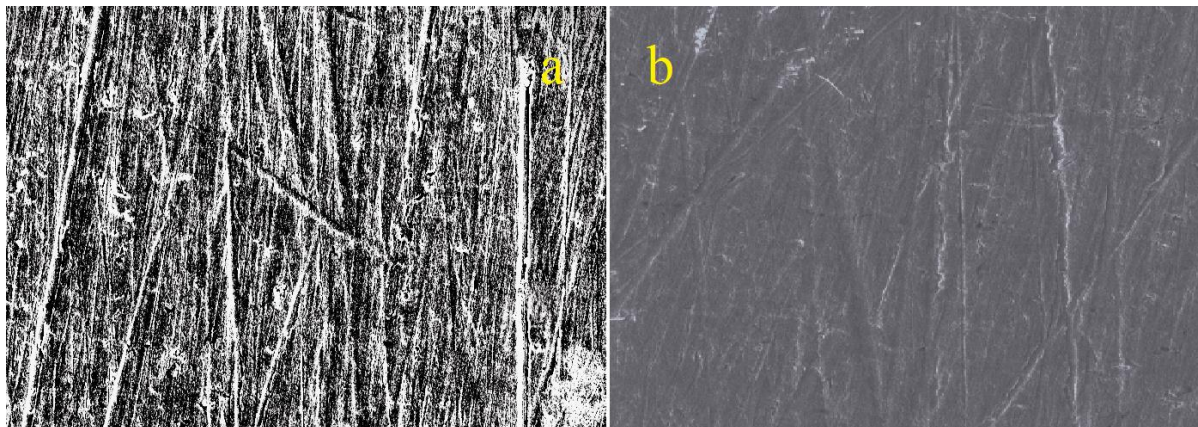


**Figure 6.** a: Mild steel surface exposed in  $1.0 \text{ mol}\cdot\text{L}^{-1}$  HCl without 2HNT inhibitor after a 5-hour exposure period; b: Mild steel surface exposed in  $1.0 \text{ mol}\cdot\text{L}^{-1}$  HCl with 2HNT inhibitor after a 5-hour exposure period.

The surface of the coupon exposed to HCl without the inhibitor exhibits evident corrosion holes, indicating substantial damage due to the aggressive nature of the acidic solution (Figure 6a). In contrast, the presence of 2HNT in the acid solution (Figure 6b) effectively mitigates the corrosion damage. The surface of the tested coupon immersed in the corrosive medium with 2HNT closely resembles the polished surface, suggesting that the inhibitor molecules form a protective film, acting as a barrier against the corrosive attack. This visual assessment aligns with the corrosion inhibition efficiency observed in the weight loss analysis, confirming the effectiveness of 2HNT in preserving the integrity of the mild steel surface in harsh acidic environments. The protective film formed by the inhibitor molecules serves as a crucial defense mechanism, demonstrating the inhibitor's potential for mitigating corrosion and preserving the structural integrity of mild steel in corrosive media.

### 3.6. Computational studies

The molecular reactivity of the investigated inhibitor, 2HNT, was probed through an exploration of the Highest Occupied Molecular Orbital (HOMO) and Lowest Unoccupied Molecular Orbital (LUMO). The HOMO energy, indicative of electron donation capability, and the LUMO energy, indicating electron acceptance ability, play pivotal roles in understanding the molecular interaction with the mild steel surface [91].

In Figure 7, the HOMO populations are concentrated around the amino, thion, and  $-\text{N}=\text{C}-$  groups, while the densities of LUMO predominantly reside around the aromatic rings. A high-energy HOMO suggests a significant ability to donate electrons to a suitable element with unoccupied molecular orbitals of low energy. This aligns with the observed physisorption mechanism, confirming the experimental findings.

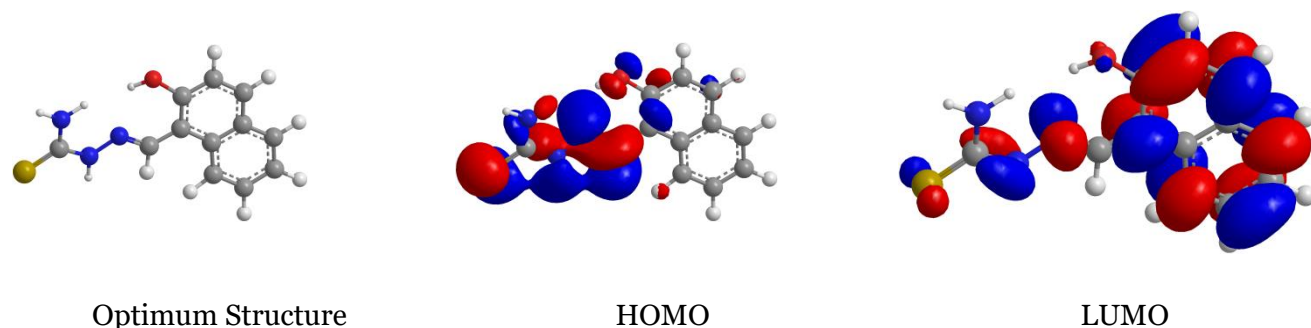


**Figure 7.** Molecular orbitals of 2HNT.

The computed quantum chemical parameters, as summarized in Table 1, further support the experimental insights. Notably, 2HNT exhibits a high HOMO energy, signifying a strong electron-donating capacity. This is consistent with the experimentally observed physisorption mechanism, where 2HNT demonstrates significant inhibition efficacy on the mild steel surface [92]. The LUMO energy, associated with electron affinity and susceptibility to nucleophilic attack, showcases 2HNT's potent electron-accepting ability. The low values of the energy gap ( $\Delta E$ ) indicate a high inhibitive efficiency, corroborating the experimental data.

**Table 1.** Computed Quantum Chemical Parameters for 2HNT.

Parameter	Value
HOMO Energy (eV)	−8.454
LUMO Energy (eV)	−3.275
Energy Gap ( $\Delta E$ ) (eV)	5.179
Hardness (eV)	2.590
Softness (eV)	0.795
Electronegativity (eV)	5.865
$\Delta N$ (number of electrons transferred)	−0.015
Dipole moment ( $\mu$ ) (Debye)	−2.3192

The low values of  $\Delta E$  and hardness, coupled with high softness, align with the experimental evidence, emphasizing the physisorption adsorption mechanism. The high HOMO energy correlates with significant inhibition efficacy, consistent with the ( $\Delta G_{\text{ads}}^0$ ) values obtained from the adsorption isotherm. Furthermore, the molecular structure's influence on adsorption is highlighted by the electron density at active sites. Electrophilic attacks are observed at sulfur, oxygen and nitrogen atoms, emphasizing these regions as active sites with strong bonding to the steel surface. Electronegativity proves crucial in predicting inhibitive efficacy. The number of electrons transferred values decrease with

increasing inhibitor electronegativity. The computed number of electrons transferred values, matching electronegativities, affirm the inhibitor's ability to donate electrons. The positive  $\Delta N$  values further validate the  $E_{\text{HOMO}}$  trends, signifying the inhibitor's electron-donating potential. In conclusion, the computational studies provide a comprehensive understanding of 2HNT's molecular reactivity, affirming its physisorption adsorption mechanism and shedding light on the critical factors influencing its corrosion inhibition efficiency on mild steel. The correlation between experimental and theoretical findings enhances the robustness of the study, underscoring the potential of 2HNT as an effective corrosion inhibitor. The dipole moment (DP) is a crucial parameter that offers insights into the polarity and charge distribution within a molecule. A dipole moment arises when there is an uneven distribution of electron density, leading to a separation of positive and negative charges, creating a dipole. In the case of 2HNT, the negative value of the dipole moment ( $-2.3192$ ) signifies a directionality of the charge distribution, indicating a net dipole moment along a specific axis. The negative sign implies that the electron distribution is skewed towards one end of the molecule. A significant dipole moment suggests a polar nature, and in the context of corrosion inhibition, it can influence the interaction between the inhibitor molecule and the metal surface. The presence of a dipole moment can enhance the adsorption of the inhibitor onto the metal surface, facilitating the formation of a protective layer.

In the scenario of 2HNT, the negative dipole moment could be associated with the orientation of functional groups within the molecule. The distribution of electron density around certain groups, such as amino, thion, and  $-\text{N}=\text{C}-$ , might contribute to the observed dipole moment. This dipole moment orientation can potentially enhance the electrostatic interactions between the inhibitor and the mild steel surface. Overall, the negative dipole moment in 2HNT suggests a polar nature and provides valuable information about the inhibitor's potential for adsorption onto the mild steel surface, contributing to its corrosion inhibition efficiency. It complements other quantum chemical parameters, enriching the understanding of the molecular features influencing the inhibitor's performance.

The computed values seem to be in good agreement with what is generally reported for similar corrosion inhibitors:

- *HOMO Energy*:  $-8.454$  eV falls within the range typically observed for effective corrosion inhibitors ( $-8.0$  eV to  $-9.0$  eV) [93].
- *LUMO Energy*:  $-3.275$  eV is slightly lower than the commonly reported range ( $-2.0$  eV to  $-3.0$  eV) [93]. This might suggest a slightly weaker electron-accepting ability compared to some other inhibitors.
- *Energy Gap ( $\Delta E$ )*:  $5.179$  eV is well within the range associated with good corrosion inhibition efficiency ( $1$  eV to  $5$  eV) [94].
- *Hardness*:  $2.590$  eV aligns with the values reported for efficient inhibitors ( $2.0$  eV to  $4.0$  eV) [95].

- *Softness*: 0.795 eV falls within the accepted range for good inhibitors (0.5 eV to 1.0 eV) [95].

The trends observed in your calculated values support the physisorption mechanism and the experimentally observed inhibition efficacy of 2HNT:

- *High HOMO energy*: This indicates a strong ability to donate electrons to the metal surface, facilitating the formation of a protective film.
- *Low  $\Delta E$  and hardness*: These suggest high reactivity and ease of electron donation, favoring adsorption.
- *High softness*: This signifies susceptibility towards the metal surface, enhancing adsorption.
- *Positive  $\Delta N$* : This confirms the electron-donating nature of the molecule, supporting the physisorption mechanism.
- *Negative dipole moment*: This implies an uneven charge distribution that could facilitate interaction with the metal surface, further promoting adsorption.

Overall, DFT results seem to be consistent with the reported literature and support the observed corrosion inhibition properties of 2HNT.

### 3.7. Mechanism of Inhibition

The corrosion inhibition mechanism of mild steel in a corrosive solution containing 2-hydroxynaphthaldehyde thiosemicarbazone (2HNT) is governed by the adsorption of 2HNT molecules onto the steel surface, facilitated by the utilization of unpaired electron pairs within 2HNT that interact with the unoccupied d-orbitals of iron (Fe) atoms present on the coupon surface [96]. Heteroatoms, particularly sulfur, oxygen, and nitrogen, play pivotal roles as reaction sites during the adsorption process, with the molecular configuration of 2HNT strategically enabling targeted and effective interaction with the metal surface. The computed adsorption free energy ( $\Delta G_{\text{ads}}^0 = -34.3$  kJ/mol) indicates a spontaneous process, suggesting that interactions between inhibitor molecules and the steel surface encompass both physisorption (electrostatic interactions) and chemisorption (chemical reaction) mechanisms [97]. As discussed earlier, the inhibitory action on mild steel primarily arises from the presence of heteroatoms, leading to the formation of a protective layer upon adsorption of inhibitor molecules onto the steel surface. Figure 8 illustrates the diverse adsorption modes adopted by the adsorbed 2HNT molecules at the steel/HCl interface [98]. In essence, the adsorption of 2HNT molecules creates a shield on the steel surface, hindering corrosive attack. The versatile nature of the inhibitive mechanism, involving both physical and chemical interactions, contributes to the robust efficacy of 2HNT as a corrosion inhibitor for mild steel in acidic environments. The orchestrated interplay between heteroatoms and the metal surface underscores the multifaceted nature of the protective layer, affirming the potential of 2HNT in corrosion prevention [99].

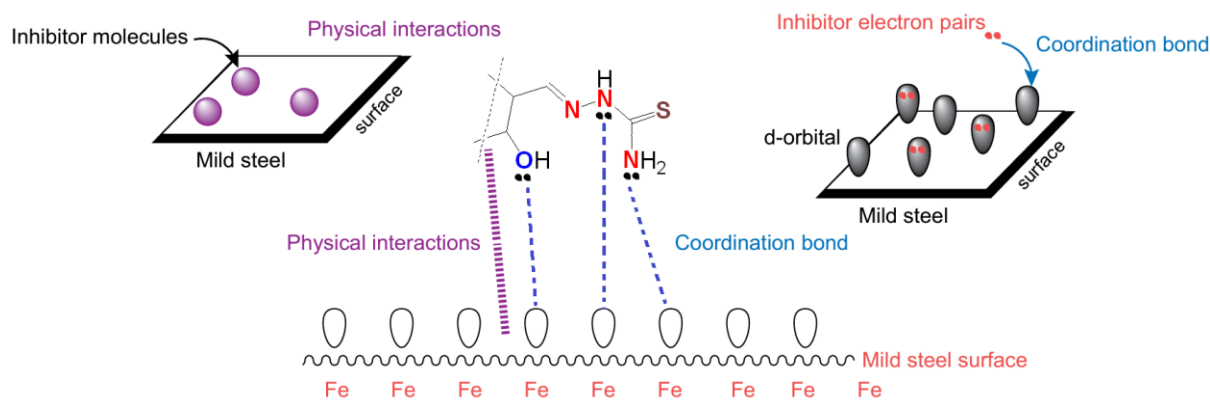


**Figure 8.** Suggested Mechanism of 2HNT Adsorption on Mild Steel in HCl Solution.

We can now deduce the inhibition mechanism by considering the following [95–100]:

- 1. Initial adsorption:** The figure illustrates the initial phase of adsorption, where 2HNT molecules approach the mild steel surface. The unoccupied *d*-orbitals of iron (Fe) atoms on the steel surface act as active sites for interaction with the unpaired electron pairs within 2HNT.
- 2. Physisorption:** Physisorption, as depicted in the diagram, involves electrostatic interactions between 2HNT molecules and the mild steel surface. The presence of heteroatoms, namely sulfur, oxygen, and nitrogen within 2HNT, plays a critical role in this process. These heteroatoms contribute to the establishment of electrostatic bonds with the metal surface, enhancing the adsorption of 2HNT molecules onto the steel substrate. Specifically, the lone pairs of electrons associated with the heteroatoms interact with positively charged sites on the metal surface, forming electrostatic bonds. This interaction results in the formation of a physical adsorption layer on the metal surface, creating an initial defense against corrosive elements present in the HCl solution. The physical adsorption layer serves as a protective barrier, preventing direct contact between the corrosive environment and the underlying metal substrate. Additionally, the presence of heteroatoms facilitates the formation of a stable adsorption layer, further enhancing the effectiveness of the inhibition process. Overall, physisorption mediated by the electrostatic interactions between 2HNT molecules and the mild steel surface provides an essential initial defense mechanism against corrosion, highlighting the significance of heteroatoms in promoting inhibitor adsorption and corrosion protection.
- 3. Chemisorption:** The diagram also suggests a chemical reaction (chemisorption) occurring between 2HNT and the mild steel surface. The strong coordination bonds formed between the unoccupied *d*-orbitals of Fe atoms and the electron-rich heteroatoms further reinforce the protective layer. The computed negative adsorption free energy ( $\Delta G_{\text{ads}}^0 = -34.3 \text{ kJ/mol}$ ) supports the spontaneous nature of this chemisorption process.

4. *Heteroatoms as reaction sites*: The heteroatoms, particularly sulfur, oxygen, and nitrogen, are highlighted as crucial reaction sites during the adsorption process. Their strategic placement enhances the specificity of the inhibitor's interaction with the metal surface, optimizing the inhibitive action.

5. *Protective layer formation*: The cumulative effect of physisorption and chemisorption processes leads to the formation of a protective layer on the mild steel surface. This layer acts as a barrier, shielding the metal from corrosive attack in the HCl solution.

In conclusion, Figure 8 provides a comprehensive visual representation of the intricate interplay between 2HNT molecules and the mild steel surface. The suggested mechanism encompasses both physical and chemical aspects, showcasing the versatility of 2HNT as a corrosion inhibitor. The proposed protective layer, fortified by electrostatic and chemical interactions, underscores the potential effectiveness of 2HNT in mitigating corrosion in acidic environments.

#### 4. Conclusion

- *Potent corrosion inhibitor*: 2-Hydroxynaphthaldehyde thiosemicarbazone (2HNT) demonstrated potent inhibition against mild steel corrosion in hydrochloric acid (HCl) solutions.
- *Experimental and theoretical analyses*: The study employed a comprehensive range of experimental and theoretical analyses to elucidate the inhibitive performance and mechanisms of 2HNT.
- *Inhibitor concentration*: A direct correlation was observed between 2HNT concentration and inhibition efficiency. Optimal inhibition (93.88%) was achieved at 500.0 ppm after a 10-hour immersion period at 303 K.
- *Dynamic nature of inhibition*: Inhibition efficiency increased gradually over time, highlighting the dynamic nature of the process. The protective film formed by 2HNT molecules effectively mitigated corrosion.
- *Temperature effects*: Temperature variations influenced inhibition efficacy, with a decrease observed at higher temperatures due to increased dynamic energy of inhibitor molecules.
- *Adsorption isotherm studies*: Langmuir isotherm modeling provided insights into the adsorption behavior of 2HNT, revealing a mixed mechanism involving both physisorption and chemisorption.
- *Molecular modeling*: HOMO and LUMO analyses confirmed the significant role of heteroatoms in the inhibitive action of 2HNT, demonstrating its versatility.
- *Surface analysis*: Surface analysis depicted the protective nature of 2HNT, with the inhibitor-formed layer effectively shielding the mild steel surface from corrosive attack.

- *Mechanism elucidation*: The suggested mechanism, detailed in Figure 8, provided a comprehensive understanding of the adsorption modes and emphasized the role of heteroatoms in the inhibitive process.
- *Overall efficacy*: This research underscores the efficacy, versatility, and stability of 2HNT as a promising corrosion inhibitor in HCl environments. The integrated approach validated the inhibitive performance and elucidated underlying mechanisms, paving the way for practical applications in corrosion mitigation strategies.

## References

1. J.I. Bhat and V.D.P. Alva, Inhibition effect of miconazole nitrate on the corrosion of mild steel in hydrochloric acid medium, *Int. J. Electrochem.*, 2011, 157576, 1–8. doi: [10.4061/2011/157576](https://doi.org/10.4061/2011/157576)
2. P.B. Raja and M.G. Sethuraman, Natural products as corrosion inhibitor for metals in corrosive media: A Review, *Mater. Lett.*, 2008, **62**, 2977–2979. doi: [10.1016/j.matlet.2007.04.079](https://doi.org/10.1016/j.matlet.2007.04.079)
3. C. Jeyaprabha, S. Sathiyarayanan, K.L.N. Phani and G. Venkatachari, Influence of poly(aminoquinone) on corrosion inhibition of iron in acid media, *Appl. Surf. Sci.*, 2005, **252**, 966–975. doi: [10.1016/j.apsusc.2005.01.098](https://doi.org/10.1016/j.apsusc.2005.01.098)
4. A.M. Abdel-Gaber, B.A. Abd-El-Nabey and M. Saadawy, The role of acid anion on the inhibition of the acidic corrosion of steel by lupine extract, *Corros. Sci.*, 2009, **51**, 1038–1042. doi: [10.1016/j.corsci.2009.03.003](https://doi.org/10.1016/j.corsci.2009.03.003)
5. K.O. Orubite and N.C. Oforka, Inhibition of corrosion of mild steel in HCl solutions by the extracts of leaves of *Nypa fruticans* Wurmb, *Mater. Lett.*, **58**, 1768–1772. doi: [10.1016/j.matlet.2003.11.030](https://doi.org/10.1016/j.matlet.2003.11.030)
6. V.V. Torres, R.S. Amado, C.F. de Sá, T.L. Fernandez, C.A.S. Riehl and A.G. Torres, Inhibitory action of aqueous coffee ground extracts on the corrosion of carbon steel in HCl solution, *Corros. Sci.*, 2011, **53**, 2385–2392. doi: [10.1016/j.corsci.2011.03.021](https://doi.org/10.1016/j.corsci.2011.03.021)
7. L.G. Trindade and R.S. Goncalves, Evidence of caffeine adsorption on a low-carbon steel surface in ethanol, *Corros. Sci.*, 2009, **51**, 1578–1583. doi: [10.1016/j.corsci.2009.03.038](https://doi.org/10.1016/j.corsci.2009.03.038)
8. A. Sharmila, A.A. Prema and P.A. Sahayaraj, Influence of *Murraya Koenigi* (curry leaves) extract on the corrosion inhibition of carbon steel in HCl solution, *Rasayan J. Chem.*, 2010, **3**, no. 1, 74–81.
9. H. Kumar, S. Yadav, R.S. Chaudhary and D. Kumar, Synergistic effect of some Antiscalants as corrosion inhibitor for an industrial cooling water system, *J. Appl. Electrochem.*, 2009, **39**, no. 8, 1339–1347. doi: [10.1007/s10800-009-9807-4](https://doi.org/10.1007/s10800-009-9807-4)
10. H. Kumar, V. Saini, D. Kumar and R.S. Chaudhary, Influence of trisodium phosphate (TSP) antiscalant on the corrosion of carbon steel in cooling water systems, *Indian J. Chem. Technol.*, 2009, **16**, 401–410.

11. H. Kumar and R.S. Chaudhary, Influence of sodium tripolyphosphate (STPP) antiscalant On the corrosion of carbon steel in cooling water systems, *Bull. Electrochem.*, 2006, **22**, no. 7, 289–296.
12. M.A. Quraishi, A. Singh, V.K. Singh, D.K. Yadav and A.K. Singh, Green approach to corrosion inhibition of mild steel in hydrochloric acid and sulphuric acid solutions by the extract of *Murraya koenigii* leaves, *Mater. Chem. Phys.*, 2010, **122**, 114–122. doi: [10.1016/j.matchemphys.2010.02.066](https://doi.org/10.1016/j.matchemphys.2010.02.066)
13. L.R. Chauhan and G. Gunasekaran, Corrosion inhibition of mild steel by plant extract in dilute HCl medium, *Corros. Sci.*, 2007, **49**, 1143–1161. doi: [10.1016/j.corsci.2006.08.012](https://doi.org/10.1016/j.corsci.2006.08.012)
14. J.C. Rocha, J.A.C.P. Gomes and E. D'Elia, Corrosion inhibition of carbon steel in hydrochloric acid solution by fruit peel aqueous extracts, *Corros. Sci.*, 2010, **52**, 2341–2348. doi: [10.1016/j.corsci.2010.03.033](https://doi.org/10.1016/j.corsci.2010.03.033)
15. A. Ostavari, S.M. Hoseinie, M. Peikari, S.R. Shadizadeh and S.J. Hashemi, Corrosion inhibition of mild steel in 1 M HCl solution by henna extract: A comparative study of the inhibition by henna and its constituents (Lawson, Gallic acid,  $\alpha$ -d-Glucose, and Tannic acid), *Corros. Sci.*, 2009, **51**, 1935–1949. doi: [10.1016/j.corsci.2009.05.024](https://doi.org/10.1016/j.corsci.2009.05.024)
16. P.C. Okafor and E.E. Ebenso, The inhibitive action of *Carica papaya* extracts on the corrosion of mild steel in acidic media and their adsorption characteristics, *Pigm. Resin Technol.*, 2007, **36**, 134–140. doi: [10.1108/03699420710748992](https://doi.org/10.1108/03699420710748992)
17. P.C. Okafor, M.E. Ikpi, I.E. Uwah, E.E. Ebenso, U.J. Ekpe and S.A. Umoren, Inhibitory action of *Phyllanthus amarus* extracts on the corrosion of mild steel in acidic media, *Corros. Sci.*, 2008, **50**, 2310–2317. doi: [10.1016/j.corsci.2008.05.009](https://doi.org/10.1016/j.corsci.2008.05.009)
18. M. Behpour, S.M. Ghoreishi, N. Soltani and M. Salavati-Niasari, The inhibitive effect of some bis-N,S-bidentate Schiff bases on corrosion behaviour of 304 stainless steel in hydrochloric acid solution, *Corros. Sci.*, 2009, **51**, 1073–1082. doi: [10.1016/j.corsci.2009.02.011](https://doi.org/10.1016/j.corsci.2009.02.011)
19. E. Naderi, A.H. Jafari, M. Ehteshamzadeh and M.G. Hosseini, Effect of carbon steel microstructures and molecular structure of two new Schiff base compounds on inhibition performance in 1 M HCl solution by EIS, *Mater. Chem. Phys.*, 2009, **115**, 852–858. doi: [10.1016/j.matchemphys.2009.03.002](https://doi.org/10.1016/j.matchemphys.2009.03.002)
20. M. Behpour, S.M. Ghoreishi, N. Soltani, M. Salavati-Niasari, M. Hamadani and A. Gandomi, Electrochemical and theoretical investigation on the corrosion inhibition of mild steel by thiosalicylaldehyde derivatives in hydrochloric acid solution, *Corros. Sci.*, 2008, **50**, no. 8, 2172–2181. doi: [10.1016/j.corsci.2008.06.020](https://doi.org/10.1016/j.corsci.2008.06.020)
21. H.D. Lece, K.C. Emregul and O. Atakol, Difference in the inhibitive effect of some Schiff base compounds containing oxygen, nitrogen and sulfur donors, *Corros. Sci.*, 2008, **50**, no. 5, 1460–1468. doi: [10.1016/j.corsci.2008.01.014](https://doi.org/10.1016/j.corsci.2008.01.014)

- 
22. R.A. Prabhu, T.V. Venkatesha, A.V. Shanbhag, G.M. Kulkarni and R.G. Kalkhambkar, Inhibition effects of some Schiff's bases on the corrosion of mild steel in hydrochloric acid solution, *Corros. Sci.*, 2008, **50**, no. 12, 3356–3362. doi: [10.1016/j.corsci.2008.09.009](https://doi.org/10.1016/j.corsci.2008.09.009)
  23. H. Keles, M. Keles, I. Dehri and O. Serindag, Adsorption and inhibitive properties of aminobiphenyl and its Schiff base on mild steel corrosion in 0.5 M HCl medium, *Colloids Surf., A*, 2008, **320**, 138–145. doi: [10.1016/j.colsurfa.2008.01.040](https://doi.org/10.1016/j.colsurfa.2008.01.040)
  24. M.K. Abbass, K.M. Raheef, I.A. Aziz, M.M. Hanoon, A.M. Mustafa, W.K. Al-Azzawi, A.A. Al-Amiery and A.A.H. Kadhum, Evaluation of 2-Dimethylaminopropionamidoantipyrine as a Corrosion Inhibitor for Mild Steel in HCl Solution: A Combined Experimental and Theoretical Study, *Prog. Color, Color. Coat.*, 2024, **17**, no. 1 1–10. doi: [10.30509/pccc.2023.167134.1216](https://doi.org/10.30509/pccc.2023.167134.1216)
  25. M.T. Mohamed, S.A. Nawi, A.M. Mustafa, F.F. Sayyid, M.M. Hanoon, A.A. Al-Amiery, A.A.H. Kadhum and W.K. Al-Azzawi, Revolutionizing Corrosion Defense: Unlocking the Power of Expired BCAA, *Prog. Color, Color. Coat.*, 2024, **17**, no. 2, 97–111. doi: [10.30509/pccc.2023.167156.1228](https://doi.org/10.30509/pccc.2023.167156.1228)
  26. E. Bayol, T. Gurten, A. Gürten and M. Erbil, Interactions of some Schiff base compounds with mild steel surface in hydrochloric acid solution, *Mater. Chem. Phys.*, 2008, **112**, 624–630. doi: [10.1016/j.matchemphys.2008.06.012](https://doi.org/10.1016/j.matchemphys.2008.06.012)
  27. C. Kustu, K.C. Emregul, E. Duzgun and O. Atakol, Schiff bases of increasing complexity as mild steel corrosion inhibitors in 2 M HCl, *Corros. Sci.*, 2007, **49**, 2800–2814. doi: [10.1016/j.corsci.2007.02.002](https://doi.org/10.1016/j.corsci.2007.02.002)
  28. K.C. Emregul and M. Hayvali, Studies on the effect of a newly synthesized Schiff base compound from phenazone and vanillin on the corrosion of steel in 2 M HCl, *Corros. Sci.*, 2006, **48**, 797–812. doi: [10.1016/j.corsci.2005.03.001](https://doi.org/10.1016/j.corsci.2005.03.001)
  29. K.C. Emregul, E. Duzgun and O. Atakol, The application of some polydentate Schiff base compounds containing aminic nitrogens as corrosion inhibitors for mild steel in acidic media, *Corros. Sci.*, 2006, **48**, 3243–3260. doi: [10.1016/j.corsci.2005.11.016](https://doi.org/10.1016/j.corsci.2005.11.016)
  30. K.C. Emregul and O. Atakol, Corrosion inhibition of iron in 1 M HCl solution with Schiff base compounds and derivatives, *Mater. Chem. Phys.*, 2004, **83**, 373–379. doi: [10.1016/j.matchemphys.2003.11.008](https://doi.org/10.1016/j.matchemphys.2003.11.008)
  31. A.Y.I. Rubaye, M.T. Mohamed, M.A.I. Al-Hamid, A.M. Mustafa, F.F. Sayyid, M.M. Hanoon, A.H. Kadhum, A.A. Alamiery and W.K. Al-Azzawi, Evaluating the corrosion inhibition efficiency of 5-(4-pyridyl)-3-mercapto-1,2,4-triazole for mild steel in HCl: insights from weight loss measurements and DFT calculations, *Int. J. Corros. Scale Inhib.*, 2024, **13**, no. 1, 185–222. doi: [10.17675/2305-6894-2024-13-1-10](https://doi.org/10.17675/2305-6894-2024-13-1-10)
  32. H.A. Sorkhabi, B. Shaabani and D. Seifzadeh, Effect of some pyrimidinic Schiff bases on the corrosion of mild steel in hydrochloric acid solution, *Electrochim. Acta*, 2005, **50**, 3446–3452. doi: [10.1016/j.electacta.2004.12.019](https://doi.org/10.1016/j.electacta.2004.12.019)

33. H.A. Sorkhabi, B. Shaabani and D. Seifzadeh, Corrosion inhibition of mild steel by some schiff base compounds in hydrochloric acid, *Appl. Surf. Sci.*, 2005, **239**, 154–164. doi: [10.1016/j.apsusc.2004.05.143](https://doi.org/10.1016/j.apsusc.2004.05.143)
34. M.N. Desai, M.B. Desai, C.B. Shah and S.M. Desai, Schiff bases as corrosion inhibitors for mild steel in hydrochloric acid solutions, *Corros. Sci.*, 1986, **26**, no. 10, 827–837. doi: [10.1016/0010-938X\(86\)90066-1](https://doi.org/10.1016/0010-938X(86)90066-1)
35. M.B. Hussein, A.M. Mustafa, M.H. Abdulkareem and A.A. Alamiery, Comparative corrosion performance of YSZ-coated Ti-13Zr-13Nb alloy and commercially pure titanium in orthopedic implants, *S. Afr. J. Chem. Eng.*, 2024, **48**, 40–54. doi: [10.1016/j.sajce.2024.01.005](https://doi.org/10.1016/j.sajce.2024.01.005)
36. H.P. Ebrahimi, J.S. Hadi, Z.A. Abdulnabi and Z. Bolandnazar, Spectroscopic, thermal analysis and DFT computational studies of salen-type Schiff base complexes, *Spectrochim. Acta, Part A*, 2014, **117**, 485–492. doi: [10.1016/j.saa.2013.08.044](https://doi.org/10.1016/j.saa.2013.08.044)
37. J. Ortega-Castro, M. Adrover, J. Frau, A. Salvà, J. Donoso and F. Muñoz, DFT studies on Schiff base formation of vitamin B6 analogues. Reaction between a pyridoxamine analogue and carbonyl compounds, *J. Phys. Chem. A*, 2010, **114**, no. 13, 4634–4640. doi: [10.1021/jp909156m](https://doi.org/10.1021/jp909156m)
38. N.O. Eddy and B.I. Ita, QSAR, DFT and quantum chemical studies on the inhibition potentials of some carbozones for the corrosion of mild steel in HCl, *J. Mol. Model.*, 2011, **17**, no. 2, 359–376. doi: [10.1007/s00894-010-0731-7](https://doi.org/10.1007/s00894-010-0731-7)
39. A. Berisha, Interactions between the aryldiazonium cations and graphene oxide: A DFT study, *J. Chem.*, 2019, 5126071. doi: [10.1155/2019/5126071](https://doi.org/10.1155/2019/5126071)
40. O. Benali, L. Larabi, M. Traisnel, L. Gengembre and Y. Harek, Electrochemical, theoretical and XPS studies of 2-mercapto-1-methylimidazole adsorption on carbon steel in 1 M HClO<sub>4</sub>, *Appl. Surf. Sci.*, 2007, **253**, no. 14, 6130–6139. doi: [10.1016/j.apsusc.2007.01.075](https://doi.org/10.1016/j.apsusc.2007.01.075)
41. A.M. Resen, M. Hanoon, R.D. Salim, A.A. Al-Amiery, L.M. Shaker and A.A.H. Kadhum, Gravimetric, theoretical, and surface morphological investigations of corrosion inhibition effect of 4-(benzoimidazole-2-yl) pyridine on mild steel in hydrochloric acid, *Koroze Ochr. Mater.*, 2020, **64**, 122–130. doi: [10.2478/kom-2020-0018](https://doi.org/10.2478/kom-2020-0018)
42. A.M. Resen, A.N. Jasim, H.S. Qasim, M.M. Hanoon, A.A. Al-Amiery, W.K. Al-Azzawi, A.M. Mustafa and F.F. Sayyid, Investigating the Corrosion Inhibition Performance of Methyl 3H-2,3,5-triazole-1-formate for Mild Steel in Hydrochloric Acid Solution: Experimental and Theoretical Insights, *Prog. Color, Color. Coat.*, 2024, **17**, no. 2, 185–205. doi: [10.30509/pccc.2023.167189.1245](https://doi.org/10.30509/pccc.2023.167189.1245)
43. N.S. Abtan, A.E. Sultan, F.F. Sayyid, A.A. Alamiery, A.H. Jaaz, T.S. Gaaz, S.M. Ahmed, A.M. Mustafa, D.A. Ali and M.M. Hanoon, Enhancing corrosion resistance of mild steel in hydrochloric acid solution using 4-phenyl-1-(phenylsulfonyl)-3-thiosemicarbazide: A comprehensive study, *Int. J. Corros. Scale Inhib.*, 2024, **13**, no. 1, 435–459. doi: [10.17675/2305-6894-2024-13-1-22](https://doi.org/10.17675/2305-6894-2024-13-1-22)

- 
44. N.S. Abtan, M.A.I. Al-Hamid, L.A. Kadhim, F.F. Sayyid, F.T.M. Noori, A. Kadum, A. Alamiery and W.K. Al-Azzawi, Unlocking the Power of 4-Acetamidoantipyrine: A Promising Corrosion Inhibitor for Preserving Mild Steel in Harsh Hydrochloric Acid Environments, *Prog. Color, Color. Coat.*, 2024, **17**, 85–96. doi: [10.30509/pccc.2023.167147.1223](https://doi.org/10.30509/pccc.2023.167147.1223)
  45. M.M. Hanoon, A.M. Resen, A.A. Al-Amiery, A.A.H. Kadhum and M.S. Takriff, Theoretical and Experimental Studies on the Corrosion Inhibition Potentials of 2-((6-Methyl-2-Ketoquinolin-3-yl)Methylene) Hydrazinecarbothioamide for Mild Steel in 1 M HCl, *Prog. Color, Color. Coat.*, 2022, **15**, no. 1, 11–23. doi: [10.30509/pccc.2020.166739.1095](https://doi.org/10.30509/pccc.2020.166739.1095)
  46. Y.M. Abdulsahib, A.J.M. Eltmimi, S.A. Alhabeeb, M.M. Hanoon, A.A. Al-Amiery, T. Allami and A.A.H. Kadhum, Experimental and theoretical investigations on the inhibition efficiency of N-(2,4-dihydroxytolueneylidene)-4-methylpyridin-2-amine for the corrosion of mild steel in hydrochloric acid, *Int. J. Corros. Scale Inhib.*, 2021, **10**, no. 3, 885–899. doi: [10.17675/2305-6894-2021-10-3-3](https://doi.org/10.17675/2305-6894-2021-10-3-3)
  47. A.K. Khudhair, A.M. Mustafa, M.M. Hanoon, A. Al-Amiery, L.M. Shaker, T. Gazz, A.B. Mohamad, A.H. Kadhum and M.S. Takriff, Experimental and Theoretical Investigation on the Corrosion Inhibitor Potential of N-MEH for Mild Steel in HCl, *Prog. Color, Color. Coat.*, 2022, **15**, 111–122. doi: [10.30509/PCCC.2021.166815.1111](https://doi.org/10.30509/PCCC.2021.166815.1111)
  48. S. Al-Baghdadi, A. Al-Amiery, T. Gaaz and A. Kadhum, Terephthalohydrazide and isophthalo-hydrazide as new corrosion inhibitors for mild steel in hydrochloric acid: Experimental and theoretical approaches, *Koroze Ochr. Mater.*, 2021, **65**, 12–22. doi: [10.2478/kom-2021-0002](https://doi.org/10.2478/kom-2021-0002)
  49. A. Alamiery, Anticorrosion effect of thiosemicarbazide derivative on mild steel in 1 M hydrochloric acid and 0.5 M sulfuric Acid: Gravimetric and theoretical studies, *Mater. Sci. Energy Technol.*, 2021, **4**, 263–273. doi: [10.1016/j.mset.2021.07.004](https://doi.org/10.1016/j.mset.2021.07.004)
  50. A.A. Alamiery, W.N.R.W. Isahak and M.S. Takriff, Inhibition of mild steel corrosion by 4-benzyl-1-(4-oxo-4-phenylbutanoyl)thiosemicarbazide: Gravimetric, adsorption and theoretical studies, *Lubricants*, 2021, **9**, 93. doi: [10.3390/lubricants9090093](https://doi.org/10.3390/lubricants9090093)
  51. M. Farsak, H. Keleş and M.A. Keleş, New Corrosion Inhibitor for Protection of Low Carbon Steel in HCl Solution, *Corros. Sci.*, 2015, **98**, 223–232. doi: [10.1016/j.corsci.2015.05.036](https://doi.org/10.1016/j.corsci.2015.05.036)
  52. I. Annon, A. Abbas, W. Al-Azzawi, M. Hanoon, A. Alamiery, W. Isahak and A. Kadhum, Corrosion inhibition of mild steel in hydrochloric acid environment using thiadiazole derivative: Weight loss, thermodynamics, adsorption and computational investigations, *S. Afr. J. Chem. Eng.*, 2022, **41**, 244–252. doi: [10.1016/j.sajce.2022.06.011](https://doi.org/10.1016/j.sajce.2022.06.011)
  53. ASTM International, Standard Practice for Preparing, Cleaning, and Evaluating Corrosion Test, 2011, 1–9.
  54. NACE International, Laboratory Corrosion Testing of Metals in Static Chemical Cleaning Solutions at Temperatures below 93°C (200°F), TM0193-2016-SG, 2000.

- 
55. M.J. Frisch, G.W. Trucks, H.B. Schlegel, G.E. Scuseria, M.A. Robb, J.R. Cheeseman, J.A. Montgomery, Jr., T. Vreven, K.N. Kudin, J.C. Burant, J.M. Millam, S.S. Iyengar, J. Tomasi, V. Barone, B. Mennucci, M. Cossi, G. Scalmani, N. Rega, G.A. Petersson, H. Nakatsuji, M. Hada, M. Ehara, K. Toyota, R. Fukuda, J. Hasegawa, M. Ishida, T. Nakajima, Y. Honda, O. Kitao, H. Nakai, M. Klene, X. Li, J.E. Knox, H.P. Hratchian, J.B. Cross, V. Bakken, C. Adamo, J. Jaramillo, R. Gomperts, R.E. Stratmann, O. Yazyev, A.J. Austin, R. Cammi, C. Pomelli, J.W. Ochterski, P.Y. Ayala, K. Morokuma, G.A. Voth, P. Salvador, J.J. Dannenberg, V.G. Zakrzewski, S. Dapprich, A.D. Daniels, M.C. Strain, O. Farkas, D.K. Malick, A.D. Rabuck, K. Raghavachari, J.B. Foresman, J.V. Ortiz, Q. Cui, A.G. Baboul, S. Clifford, J. Cioslowski, B.B. Stefanov, G. Liu, A. Liashenko, P. Piskorz, I. Komaromi, R.L. Martin, D.J. Fox, T. Keith, M.A. Al-Laham, C.Y. Peng, A. Nanayakkara, M. Challacombe, P.M.W. Gill, B. Johnson, W. Chen, M.W. Wong, C. Gonzalez and J.A. Pople, *Gaussian 03, Revision B. 05*, Gaussian, Inc., Wallingford, CT, 2004.
56. T. Koopmans, Ordering of wave functions and eigen-energies to the individual electrons of an atom, *Physica*, 1934, **1**, no. 1–6, 104–113 (in German). doi: [10.1016/S0031-8914\(34\)90011-2](https://doi.org/10.1016/S0031-8914(34)90011-2)
57. S. Zhang, W. Lei, M. Xia and F. Wang, QSAR study on N-containing corrosion inhibitors: quantum chemical approach assisted by topological index, *J. Mol. Struct.: THEOCHEM*, 2005, **732**, no. 1–3, 173–182. doi: [10.1016/j.theochem.2005.02.091](https://doi.org/10.1016/j.theochem.2005.02.091)
58. L.O. Olasunkanmi, I.B. Obot, M.M. Kabanda and E.E. Ebenso, Some quinoxalin-6-yl derivatives as corrosion inhibitors for mild steel in hydrochloric acid: Experimental and theoretical studies, *J. Phys. Chem. C*, 2015, **119**, 16004–16019. doi: [10.1021/acs.jpcc.5b03285](https://doi.org/10.1021/acs.jpcc.5b03285)
59. A.M. Resen, M.M. Hanoon, W.K. Alani, A. Kadhim, A.A. Mohammed, T.S. Gaaz, A.A.H. Kadhum, A.A. Al-Amiery and M.S. Takriff, Exploration of 8-piperazine-1-ylmethylumbelliferone for application as a corrosion inhibitor for mild steel in hydrochloric acid solution, *Int. J. Corros. Scale Inhib.*, 2021, **10**, no. 1, 368–387. doi: [10.17675/2305-6894-2021-10-1-21](https://doi.org/10.17675/2305-6894-2021-10-1-21)
60. M. Chen, S. Lu, G. Yuan, S. Yang and X. Du, Synthesis and Antibacterial Activity of some Heterocyclic  $\beta$ -Enamino Ester Derivatives with 1,2,3-triazole, *Heterocycl. Commun.*, 2000, **6**, no. 5, 421–426. doi: [10.1515/HC.2000.6.5.421](https://doi.org/10.1515/HC.2000.6.5.421)
61. Y.A. Al-Soud, M.N. Al-Dweri and N.A. Al-Masoudi, Synthesis, antitumor and antiviral properties of some 1,2,4-triazole derivatives, *Farmaco*, 2004, **59**, no. 10, 775–783. doi: [10.1016/j.farmac.2004.05.006](https://doi.org/10.1016/j.farmac.2004.05.006)
62. M. Ur-Rahman, Y. Mohammad, K.M. Fazili, K.A. Bhat and T. Ara, Synthesis and biological evaluation of novel 3-O-tethered triazoles of diosgenin as potent antiproliferative agents, *Steroids*, 2017, **118**, 1–8. doi: [10.1016/j.steroids.2016.11.003](https://doi.org/10.1016/j.steroids.2016.11.003)
63. M. Huang, Z. Deng, J. Tian and T. Liu, Synthesis and biological evaluation of salinomycin triazole analogues as anticancer agents, *Eur. J. Med. Chem.*, 2017, **127**, 900–908. doi: [10.1016/j.ejmech.2016.10.067](https://doi.org/10.1016/j.ejmech.2016.10.067)

- 
64. K. Karrouchi, L. Chemlal, J. Taoufik, Y. Cherrah, S. Radi, M.El Abbes Faouzi and M. Ansar, Synthesis, antioxidant and analgesic activities of Schiff bases of 4-amino-1,2,4-triazole derivatives containing a pyrazole moiety, *Ann. Pharm. Fr.*, 2016, **74**, no. 6, 431–438. doi: [10.1016/j.pharma.2016.03.005](https://doi.org/10.1016/j.pharma.2016.03.005)
65. O.A. Goncharova, A.Yu. Luchkin, N.N. Andreev, N.P. Andreeva and S.S. Vesely, Triazole derivatives as chamber inhibitors of copper corrosion, *Int. J. Corros. Scale Inhib.*, 2018, **7**, no. 4, 657–672. doi: [10.17675/2305-6894-2018-7-4-12](https://doi.org/10.17675/2305-6894-2018-7-4-12)
66. K.F. Khaled, Molecular simulation, quantum chemical calculations and electrochemical studies for inhibition of mild steel by triazoles, *Electrochim. Acta*, 2008, **53**, no. 9, 34843492. doi: [10.1016/j.electacta.2007.12.030](https://doi.org/10.1016/j.electacta.2007.12.030)
67. S. Maddila, R. Pagadala and S. Jonnalagadda, 1,2,4-Triazoles: A Review of Synthetic Approaches and the Biological Activity, *Lett. Org. Chem.*, 2013, **10**, no. 10, 693–714. doi: [10.2174/157017861010131126115448](https://doi.org/10.2174/157017861010131126115448)
68. L.P. Guan, Q.H. Jin, G.R. Tian, K.Y. Chai and Z.S. Quan, Synthesis of some quinoline-2(1H)-one and 1,2,4-triazolo[4,3-a] quinoline derivatives as potent anticonvulsants, *J. Pharm. Pharm. Sci.*, 2007, **10**, no. 3, 254–262.
69. R. Gujjar, A. Marwaha, F.El Mazouni, J.K. White, K.L. White, S. Creason, D.M. Shackelford, J. Baldwin, W.N. Charman, F.S. Buckner, S. Charman, P.K. Rathod and M.A. Phillips, Identification of a metabolically stable triazolopyrimidine-based dihydroorotate dehydrogenase inhibitor with antimalarial activity in mice, *J. Med. Chem.*, 2009, **52**, no. 7, 1864–1872. doi: [10.1021/jm801343r](https://doi.org/10.1021/jm801343r)
70. B. Hammouti, A. Zarrouk, S.S. Al-Deyab and I. Warad, Temperature Effect, Activation Energies and Thermodynamics of Adsorption of ethyl 2-(4-(2-ethoxy-2-oxoethyl)-2-pTolylquinoxalin-1(4H)-yl) Acetate on Cu in HNO<sub>3</sub>, *Orient. J. Chem.*, 2011, **27**, no. 1, 23–31.
71. E.A. Noor and A.H. Al-Moubaraki, Thermodynamic study of metal corrosion and inhibitor adsorption processes in mild steel/1-methyl-4[4'-(X)-styryl] pyridinium iodides/hydrochloric acid systems, *Mater. Chem. Phys.*, 2008, **110**, 145–154. doi: [10.1016/j.matchemphys.2008.01.028](https://doi.org/10.1016/j.matchemphys.2008.01.028)
72. O. Benali, L. Larabi, M. Traisnel, L. Gengembre and Y. Harek, Electrochemical, theoretical and XPS studies of 2-mercapto-1-methylimidazole adsorption on carbon steel in 1 M HClO<sub>4</sub>, *Appl. Surf. Sci.*, 2007, **253**, no. 14, 6130–6139. doi: [10.1016/j.apsusc.2007.01.075](https://doi.org/10.1016/j.apsusc.2007.01.075)
73. P. Muthukrishnan, B. Jeyaprabha and P. Prakash, Adsorption and corrosion inhibiting behavior of *Lannea coromandelica* leaf extract on mild steel corrosion, *Arab. J. Chem.*, 2017, **10**, S2343–S2354. doi: [10.1016/j.arabjc.2013.08.011](https://doi.org/10.1016/j.arabjc.2013.08.011)
74. M. Hadizadeh, L. Yang, G. Fang, Z. Qiu and Z. Li, Mobility and Solvation Structure of Hydroxyl Radical in a Water Nanodroplet: A Born-Oppenheimer Molecular Dynamics Study, *Phys. Chem. Chem. Phys.*, 2021, **23**, 14628–14635. doi: [10.1039/D1CP01830B](https://doi.org/10.1039/D1CP01830B)
75. M. Hadizadeh and M. Hamadani, Adsorption of toxic gases by an open nanocone coupled with an iron atom, *Bulg. Chem. Commun.*, 2014, **46**, no. 3, 576–579.

- 
76. O.A. Goncharova, A.Yu. Luchkin, Yu.I. Kuznetsov, N.N. Andreev, N.P. Andreeva and S.S. Vesely, Octadecylamine, 1,2,3-benzotriazole and a mixture thereof as chamber inhibitors of steel corrosion, *Int. J. Corros. Scale Inhib.*, 2018, **7**, no. 2, 203–212. doi: [10.17675/2305-6894-2018-7-2-7](https://doi.org/10.17675/2305-6894-2018-7-2-7)
77. Ya.G. Avdeev, D.S. Kuznetsov, M.V. Tyurina and M.A. Chekulaev, Protection of nickel-chromium steel in sulfuric acid solution by a substituted triazole, *Int. J. Corros. Scale Inhib.*, 2015, **4**, no. 2, 146–161. doi: [10.17675/2305-6894-2015-4-1-146-161](https://doi.org/10.17675/2305-6894-2015-4-1-146-161)
78. I.A. Arkhipushkin, Yu.E. Pronin, S.S. Vesely and L.P. Kazansky, Electrochemical and XPS study of 2-mercaptobenzothiazole nanolayers on zinc and copper surface, *Int. J. Corros. Scale Inhib.*, 2014, **3**, no. 2, 78–88. doi: [10.17675/2305-6894-2014-3-2-078-088](https://doi.org/10.17675/2305-6894-2014-3-2-078-088)
79. V.A. Trapeznikov, I.N. Shabanova, A.V. Kholzakov and A.G. Ponomaryov, Studies of transition metal melts by X-ray electron magnetic spectrometer, *J. Electron Spectrosc. Relat. Phenom.*, 2004, **137–140**, 383–385. doi: [10.1016/j.elspec.2004.02.115](https://doi.org/10.1016/j.elspec.2004.02.115)
80. I.N. Shabanova, R.A. Nurullina, V.A. Trapeznikov and J.G. Manakov, Electronic magnet spectrometer, RU Patent 2338295 C1, 2008, IPC H01J49/48 (in Russian). <https://patenton.ru/patent/RU2338295C1/en>
81. N.A. Gladkikh, M.A. Maleeva, L.B. Maksaeva, M.A. Petrunin, A.A. Rybkina, T.A. Yurasova, A.I. Marshakov and R.Kh. Zalavutdinov, Localized dissolution of carbon steel used for pipelines under constant cathodic polarization conditions. Initial stages of defect formation, *Int. J. Corros. Scale Inhib.*, 2018, **7**, no. 4, 683–696. doi: [10.17675/2305-6894-2018-7-4-14](https://doi.org/10.17675/2305-6894-2018-7-4-14)
82. Yu.I. Kuznetsov, N.N. Andreev and S.S. Vesely, Why we reject papers with calculations of inhibitor adsorption based on data on protective effects, *Int. J. Corros. Scale Inhib.*, 2015, **4**, no. 2, 108–109.
83. M. Sobhi, M. Abdallah and K.S. Khairou, Sildenafil citrate (Viagra) as a corrosion inhibitor for carbon steel in hydrochloric acid solutions, *Monatsh. Chem.*, 2012, **143**, 1379. doi: [10.1007/s00706-011-0710-4](https://doi.org/10.1007/s00706-011-0710-4)
84. K.F. Khaled, Molecular simulation, quantum chemical calculations and electrochemical studies for inhibition of mild steel by triazoles, *Electrochim. Acta*, 2008, **53**, no. 9, 34843492. doi: [10.1016/j.electacta.2007.12.030](https://doi.org/10.1016/j.electacta.2007.12.030)
85. R. Haldhar, D. Prasad, A. Saxena and P. Singh, *Valeriana Wallichii* Root Extract as a Green & Sustainable Corrosion Inhibitor for Mild Steel in Acidic Environments: Experimental and Theoretical Study, *Mater. Chem. Front.*, 2018, **2**, 1225–1237. doi: [10.1039/C8QM00120K](https://doi.org/10.1039/C8QM00120K)
86. L.O. Olasunkanmi, I.B. Obot, M.M. Kabanda and E.E. Ebenso, Some quinoxalin-6-yl derivatives as corrosion inhibitors for mild steel in hydrochloric acid: Experimental and theoretical studies, *J. Phys. Chem. C*, 2015, **119**, 16004–16019. doi: [10.1021/acs.jpcc.5b03285](https://doi.org/10.1021/acs.jpcc.5b03285)
87. M. Stern and A.L. Geary, Electrochemical polarization, I. theoretical analysis of the shape of polarisation curves, *J. Electrochem. Soc.*, 1957, **104**, 56–63. doi: [10.1149/1.2428496](https://doi.org/10.1149/1.2428496)

- 
88. M.A. Amin, M.A. Ahmed, H.A. Arida, F. Kandemirli, M. Saracoglu, T. Arslan and M.A. Basaran, Monitoring corrosion and corrosion control of iron in HCl by non-ionic surfactants of the TRITON-X series–part III. Immersion time effects and theoretical studies, *Corros. Sci.*, 2011, **53**, 1895–1909. doi: [10.1016/j.corsci.2011.02.007](https://doi.org/10.1016/j.corsci.2011.02.007)
89. F.G. Hashim, T.A. Salman, S.B. Al-Baghdadi, T. Gaaz and A.A. Al-Amiery, Inhibition effect of hydrazine-derived coumarin on a mild steel surface in hydrochloric acid, *Tribologia*, 2020, **37**, no. 3–4, 45–53. doi: [10.30678/fjt.95510](https://doi.org/10.30678/fjt.95510)
90. A. Al-Amiery, L.M. Shaker, A.A.H. Kadhum and M.S. Takriff, Synthesis, characterization and gravimetric studies of novel triazole-based compound, *Int. J. Low-Carbon Technol.*, 2020, **15**, no. 2, 164–170. doi: [10.1093/ijlct/ctz067](https://doi.org/10.1093/ijlct/ctz067)
91. O. Tapia, Solvent effect theories: Quantum and classical formalisms and their applications in chemistry and biochemistry, *J. Math. Chem.*, 1992, **10**, no. 1, 139–181. doi: [10.1007/BF01169173](https://doi.org/10.1007/BF01169173)
92. B.I.A. Simkin and I.I. Sheikhet, *Quantum chemical and statistical theory of solutions: a computational approach*, Ellis Horwood, London, 1995.
93. A.Y. Rubaye, A.A. Abdulwahid, S.B. Al-Baghdadi, A.A. Al-Amiery, A.A. Kadhum and A.B. Mohamad, Cheery sticks plant extract as a green corrosion inhibitor complemented with LC-EIS/MS spectroscopy, *Int. J. Electrochem. Sci.*, 2015, **10**, no. 10, 8200-9.
94. M. Dalia, A.K. Al-Okbi, M.M. Hanon, K.S. Rida, A. Alkaim, A. Al-Amiery, A. Kadhum and A. Kadhum, Carbethoxythiazole corrosion inhibitor: as an experimentally model and DFT theory, *J. Eng. Appl. Sci.*, 2018, **13**, no. 11, 3952–3959. doi: [10.3923/JEASCI.2018.3952.3959](https://doi.org/10.3923/JEASCI.2018.3952.3959)
95. M.M. Hanoon, A.M. Resen, L.M. Shaker, A.A.H. Kadhum and A.A. Al-Amiery, Corrosion investigation of mild steel in aqueous hydrochloric acid environment using N-(naphthalen-1-yl)-1-(4-pyridinyl)methanimine complemented with antibacterial studies, *Biointerface Res. Appl. Chem.*, 2021, **11**, no. 2, 9735–9743. doi: [10.33263/BRIAC112.97359743](https://doi.org/10.33263/BRIAC112.97359743)
96. A. Chaouiki, M. Chafiq, A.H. Al-Moubaraki, M. Bakhouch, M. El Yazidi and Y.G. Ko, Electrochemical behavior and interfacial bonding mechanism of new synthesized carbocyclic inhibitor for exceptional corrosion resistance of steel alloy: DFTB, MD and experimental approaches, *Arabian J. Chem.*, 2022, **15**, no. 12, 104323. doi: [10.1016/j.arabjc.2022.104323](https://doi.org/10.1016/j.arabjc.2022.104323)
97. H. Liu, B. Fan, Z. Liu, X. Zhao, B. Yang, X. Zheng and H. Hao, Electronic effects on protective mechanism of electropolymerized coatings based on N-substituted aniline derivatives for mild steel in saline solution, *J. Ind. Eng. Chem.*, 2021, **106**, 297–310. doi: [10.1016/j.jiec.2021.11.004](https://doi.org/10.1016/j.jiec.2021.11.004)
98. S. Song, H. Yan, M. Cai, Y. Huang, X. Fan and M. Zhu, Constructing mechanochemical durable superhydrophobic composite coating towards superior anticorrosion, *Adv. Mater. Technol.*, 2022, **7**, no. 6, 2101223. doi: [10.1002/admt.202101223](https://doi.org/10.1002/admt.202101223)

- 
99. A. Pistone, C. Scolaro and A. Visco, Mechanical properties of protective coatings against marine fouling: A review, *Polymers*, 2021, **13**, no. 2, 173. doi: [10.3390/polym13020173](https://doi.org/10.3390/polym13020173)
100. H. Wu, H. Lei, Y.F. Chen and J. Qiao, Comparison on corrosion behaviour and mechanical properties of structural steel exposed between urban industrial atmosphere and laboratory simulated environment, *Constr. Build. Mater.*, 2019, **211**, 228–243. doi: [10.1016/j.conbuildmat.2019.03.207](https://doi.org/10.1016/j.conbuildmat.2019.03.207)

